Journal of Atmospheric and Solar-Terrestrial Physics 122 (2015) 26–33

Contents lists available at ScienceDirect

Journal of Atmospheric and Solar-Terrestrial Physics

journal homepage: www.elsevier.com/locate/jastp

Correlation between solar activity and the local temperature of Antarctica during the past 11,000 years

X.H. Zhao *, X.S. Feng *

SIGMA Weather Group, State Key Laboratory of Space Weather, Center for Space Science and Applied Research, Chinese Academy of Sciences, Beijing 100190, China

ARTICLE INFO

Article history:
Received 29 April 2014
Received in revised form
13 November 2014
Accepted 15 November 2014
Available online 20 November 2014

Keywords:
Solar activity
Climate change
Periodicity
Wavelet coherence

ABSTRACT

The solar impact on the Earth's climate change is a long topic with intense debates. Based on the reconstructed data of solar sunspot number (SSN), the local temperature in Vostok (T), and the atmospheric CO_2 concentration data of Dome Concordia, we investigate the periodicities of solar activity, the atmospheric CO_2 and local temperature in the inland Antarctica as well as their correlations during the past 11,000 years before AD 1895. We find that the variations of SSN and T have some common periodicities, such as the 208 year (yr), 521 yr, and ~1000 yr cycles. The correlations between SSN and T are strong for some intermittent periodicities. However, the wavelet analysis demonstrates that the relative phase relations between them usually do not hold stable except for the millennium-cycle component. The millennial variation of SSN leads that of T by 30–40 years, and the anti-phase relation between them keeps stable nearly over the whole 11,000 years of the past. As a contrast, the correlations between CO_2 and T are neither strong nor stable. These results indicate that solar activity might have potential influences on the long-term change of Vostok's local climate during the past 11,000 years before modern industry.

1. Introduction

Global warming is one of the hottest as well as the most debatable issues in both the scientific and public community at present. Many factors are thought to be the potential reasons to cause the present warming, such as atmospheric circulation, surface conditions of the Earth, human activities, solar activities and volcanic activities. Solar activities, often denoted by the sunspot number (SSN), refer to transient processes occurring in solar atmosphere and lower layers. They have been believed to be the natural force to drive the long-term change of the Earth's climate for a long time. As early as 1801, Herschel suggested that solar activity may play a role in the variability of the Earth's climate, and found that the rainfall was reduced on the Earth when SSN was few on the Sun (Herschel, 1801). Many subsequent papers provided more and more evidences on good correlations between solar activities and some climate indexes. For example, the "Maunder Minimum" of solar activity (AD 1645–AD 1715) coincided well with the coldest excursion of the "Little Ice Age" (Eddy, 1976). Climate elements (air temperature, sea-level, and so on) were found to have some solar-cycle signals (e.g., Currie, 1979). Strong correlations were uncovered between solar activities and the northern hemisphere temperature, revealing a direct solar influence on the Earth's climate (Christensen and Lassen, 1991; Lean et al., 1995).

Some studies argued that the green-house gases released into the atmosphere since the industrial revolution are the main reason for the global warming in the 20th century (e.g., Hegerl et al., 2007). However, the Earth's temperature shows a big variability before the period of anthropogenic influence, such as the Medieval Warm Period (AD 900–AD 1300) and the Little Ice Age (AD 1550–AD 1850). This demonstrates that natural forces without modern human activities can also lead to strong climate variability, and their effects should not be neglected in the present climate change. New evidences reveal that solar activity may play a large role in regulating the climate features of the Earth (Bond et al., 2001; Usoskin et al., 2005; Scafetta and West, 2006; Svensmark, 2007; Singer, 2008; Eichler et al., 2009; Ziskin and Shaviv, 2012). Therefore, it is still valuable to investigate the influence of solar variability on the Earth's climate change, especially on long time scales. Temperature is one of the most fundamental and longest-recorded climate elements. This paper will probe the periodicities of the variations of both solar activity and the Earth's local temperature, and investigate their correlations during the past 11,000 years.

* Corresponding authors.
E-mail addresses: xhzhao@spaceweather.ac.c (X.H. Zhao), fengx@spaceweather.ac.cn (X.S. Feng).

http://dx.doi.org/10.1016/j.jastp.2014.11.004
1364-6826/

2. Data and methodology

SSN is the parameter most widely used to denote the solar activity level. The time series of directly-observed SSN can only be extended back to ~AD 1610 when the telescope was invented, and the well-calibrated systematic measurements of SSN started 100 years later (Eddy, 1976; Usoskin et al., 2013). The time scale of the whole SSN data covers roughly 400 years. In order to get solar activity data of much longer time, reconstructed data is a good proxy. The reconstructed SSN data of Solanki et al. (2004) are adopted in this study. They were based on the dendrochronologically dated radiocarbon concentrations as well as physics-based models for each process connecting the radiocarbon concentration with SSN. The reconstructed data start from BC 9455 and end at AD 1895, coving 11,400 years in the past with a uniform temporal resolution of 10 years.

The modern continuous measurements of the Earth's surface temperature began from AD 1880. To get the data over 10,000 years, the Antarctic local temperatures, reconstructed from the stable isotope data of the Vostok ice cores (Petit et al., 1999; 2001), are adopted in this paper. In their reconstructions, the temperatures were calculated using a deuterium/temperature gradient of $\delta D‰/°C$. Their results provide a data series of the local temperature at Vostok station in East Antarctica during the past 420,000 years with a non-uniform temporal resolution. In order to align with the SSN data, we compute the interpolations of the temperature data at fixed interval of 10 years, and select the section from BC 9455 to AD 1895 as the temperature data (T) used in this paper.

As the green-house gases are thought to be associated with the Earth's temperature change, we also adopt the atmospheric CO_2 concentration data obtained from the Dome Concordia and Dronning Maud Land (Antarctica) ice cores (Monnin et al., 2004). The "European Project for Ice Coring in Antarctica" (EPICA) Dome C ice core data provide the CO_2 concentration in the past 20,000 years (backward from AD 1777) with a non-uniform temporal resolution. Similarly, we compute the interpolations of the CO_2 data at fixed interval of 10 years, and select the section from BC 9455 to AD 1775 as the CO_2 data used in this study. In the following, the term "CO_2" also refers to the atmospheric CO_2 concentration that we used in this study.

The periodicities of the time series as well as their correlations are investigated in this paper to reveal the possible link between the solar-climate relations on long time scales. The Lomb–Scargle periodogram method (Lomb, 1976; Scargle, 1982) is adopted to reconstruct the periodicities of the time series. This method is superior to traditional Fourier transform due to its applicability to the incomplete or unevenly sampled time series. It succeeds in extracting useful signals from noise, and has been widely used in geophysical researches. As to the correlation analysis, the wavelet

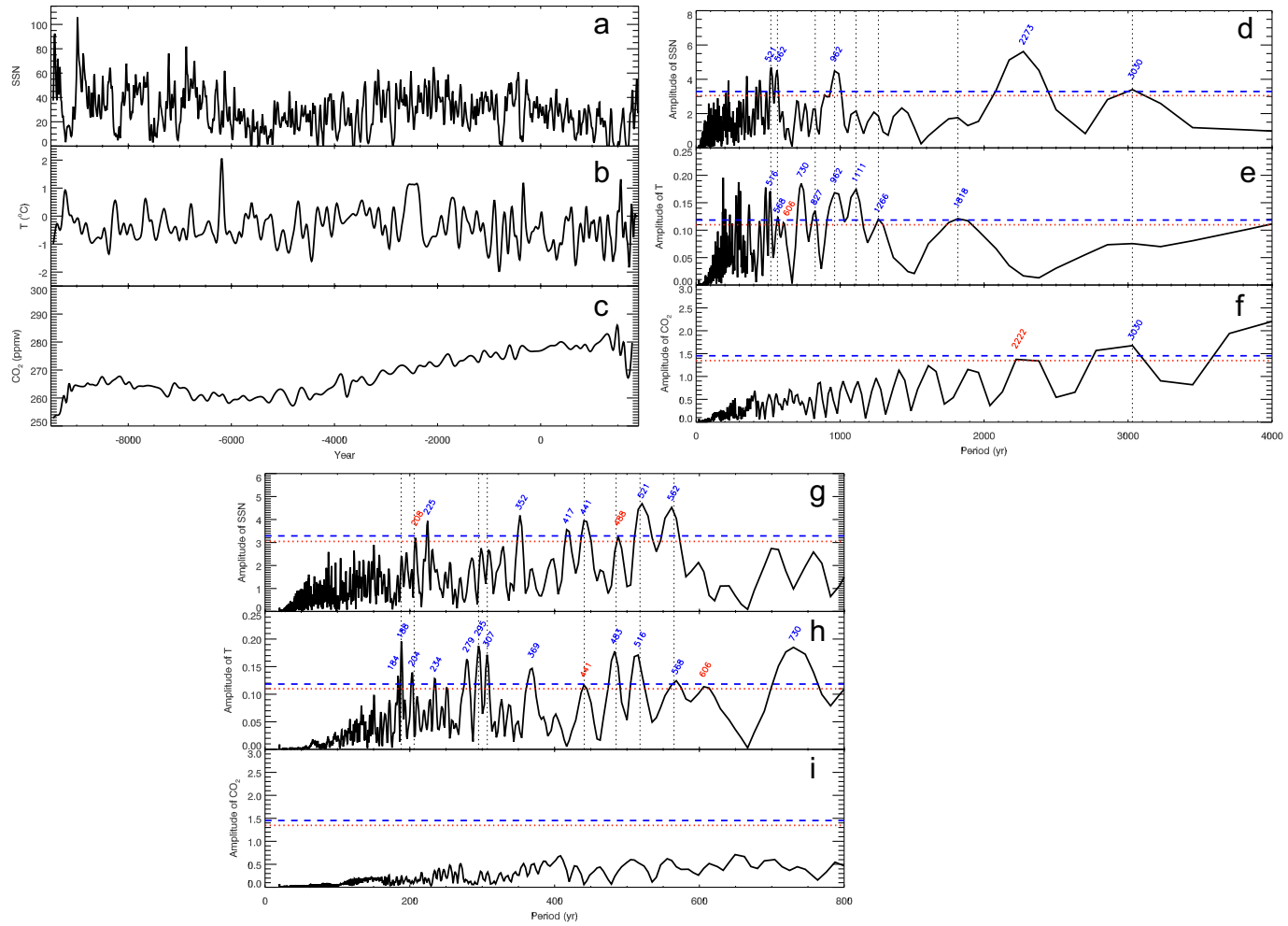

Fig. 1. Variations of SSN, T, CO_2 and their Lomb–Scargle periodograms. (a) Time series of SSN during BC 9455–AD 1895, (d) the Lomb–Scargle periodogram of SSN, (g) zoom-in of (d). (b) Time series of T during BC 9455–AD 1895, (e) the Lomb–Scargle periodogram of T, (h) zoom-in of (e). (c) Time series of CO_2 during BC 9455–AD 1775, (f) the Lomb–Scargle periodograms of CO_2, (i) zoom-in of (f). The horizontal dashed and dotted lines denote the 99%, 95% confidence levels, respectively. The vertical dotted lines indicate the coincidence of the spectral peaks of different series. The periods with stronger spectral peaks are annotated (in unit of yr) in the Lomb–Scargle periodgrams.

coherence method (Torrence and Compo, 1998; Grinsted et al., 2004) will be used to examine the relations in time frequency space between the time series of solar activity, atmospheric CO_2 concentration and temperature in the inland Antarctic stations.

3. Analysis results

3.1. Periodicities

We first study the periodicities of SSN, the local temperature T and atmospheric CO_2 concentration during the past 11,000 years. Fig. 1 shows the variations of SSN, T, CO_2 and their Lomb–Scargle periodograms in (a)–(i), respectively. The Lomb–Scargle spectrum identifies a number of distinct periodicities. It can be seen that solar activity represented by SSN has the following periodicities over the 95% confidence level during BC 9455–AD 1895: 208, 225, 352, 417, 441,488, 521, 562, 962, 2273, and 3030 years (yr) as demonstrated by the number on each spectral peak in Fig. 1(d) and (g). Most periodicities of SSN found here are consistent with previous studies. For example, the 208 yr period is referred to as the Suess or de Vries cycle (Suess, 1980), which has been confirmed by recent studies on cosmic rays (Abreu et al., 2012; McCracken et al., 2013a; 2014; Steinhilber and Beer, 2013). The 960 yr period is named as the Eddy cycle of solar activity (Abreu et al., 2012; McCracken et al., 2013a; 2014). The 2273 yr period is named as the Hallstatt cycle (Steinhilber et al., 2010; Abreu et al., 2012; Steinhilber and Beer, 2013; McCracken et al., 2013b; 2014). The periods of 352 yr and 521 yr have also been reported in solar activity through analysis of the cosmogenic data (McCracken et al., 2013a; 2014). The consistency between the SSN periodicities found here with those obtained in other studies demonstrates that they are fundamental features of solar variability. This consistency, on the other hand, witnesses the rationality and reliability of both the data and analysis methods used here. High frequency periodicities, such as the Schwabe period (11 yr), have not been found in the power spectrum due to the low temporal resolution (10 years) of the reconstructed SSN data.

The variation of Vostok temperature (T) during BC 9455–AD 1895 has significant periodicities over the 95% confidence level of 184, 188, 204, 234, 279, 295, 307, 369, 441, 483, 516, 568, 606, 730, 827, 962, 1111, 1266, and 1818 yr. The 234 yr period has been found in the temperature recorded from six Central European stations (Lüdecke et al., 2013), and the 184 yr, 516 yr periods are also very close to the 182 yr, 512 yr periods found in Lüdecke et al. (2013). Comparing panel 1(d) to 1(e) and 1(g) to 1(h) in Fig. 1, we can know that the periodograms of SSN and T are similar. The vertical dotted lines indicate the coincidence of the spectral peaks of these two time series. The common periodicities between them are 208 (204), 441, 488 (483), 521 (516), 562 (568), and 962 yr. Particularly, the Eddy cycle (962 yr) of solar activity is found in the local temperature's variation of Vostok. The common periodicities between them indicate that the variation of Vostok temperature might be modulated by solar activity on scales of these cycle lengths.

As to the atmospheric CO_2 concentration, its variation during BC 9455–AD 1775 has only two prominent periodicities, i.e., the 3030 yr period higher than the 99% confidence level, and the 2222 yr period higher than the 95% confidence level. The periodogram of CO_2 is also evidently different from those of SSN and T. Therefore, the periodic variations of CO_2 shorter than two millennia have no notable resonance with the local temperature and/or with solar activity during the past 11,000 years directly seen from the periodograms. The 3030 yr period is also found in SSN. However, we should be cautious about this coincidence as the total data only covers three cycles of this periodic component.

3.2. Wavelet coherence

Both solar activities and the Earth's climate change involve extremely complicate systems. Proximities of periodicities in such complicated series cannot prove their relation without an analysis of the correlation, especially the relative phase, between them. Here, we use the Wavelet Coherence (WTC) tool developed by Grinsted et al. (2004) to compute the correlations between SSN, T and CO_2. The wavelet coherence measures how coherent the cross wavelet transform between series is along time and frequency. It is an expansion of the correlation analysis into time and frequency domains, and provides the relative phase between signal's variations.

Fig. 2(a) gives the contour of the squared wavelet coherence between SSN and T. The regions inside the "cone of influence" (COI) where edge effects become significant are removed from the figure. The 95% confidence level against red noise, estimated by Monte Carlo methods, is shown as a thick contour. There are isolated "islands" where the wavelet coherence higher than the 95% confidence level, especially during the period bands of 64–512 yr and near 1024 yr. This demonstrates that the overall correlation between SSN and T is not evident at first glance. Strong correlations only appear at certain frequency band and/or during specific time. What's more, we need to be very careful in interpreting these coherence peaks. If there are some kinds of connections between the time series at certain frequency, the wavelet coherence between them needs to be phase-locked besides high correlation. Phase-locked means that the relative phase angles of the signals are a constant versus time. The relative phases between SSN and T are shown as arrows in Fig. 2(a) with the arrow direction pointing right for in-phase, pointing left for anti-phase, pointing straight down when SSN leading T by 90°, and pointing straight up when SSN lagging T by 90°. It is easily seen from Fig. 2 (a) that the relative phases are not locked (i.e. arrows pointing to all directions) in the period band of ~64 to 512 yr although the wavelet coherence is high in these regions. While for the period of 1024 yr and 2048 yr, the relative phases are well locked with arrows pointing to one direction during the majority of time.

In order to get the quantitative description about the relationship between coherence/phase and period, the time-integrated global quantities are adopted. Here, we define the global wavelet coherence (C_g) as the average of the squared wavelet coherence along time outside COI. For a set of phase angles θ_i ($i=1,2,\ldots n$), their circular mean values (θ_{ave}) and corresponding phase angle strength (S_θ) are defined as (Grinsted et al., 2004):

$$\theta_{ave} = arg\left(\sum_{i=1}^{n} \cos\theta_i, \ \sum_{i=1}^{n} \sin\theta_i \right) \quad (1)$$

$$S_\theta = \frac{\sqrt{(\sum_{i=1}^{n} \sin\theta_i)^2 + (\sum_{i=1}^{n} \cos\theta_i)^2}}{n} \quad (2)$$

The value of S_θ lies in the range of [0, 1], and can be used to measure the variance of the phase angles. Low value of S_θ corresponds to large variances of θ_i, while high value of S_θ corresponds to few variances of θ_i. Fig. 2(b) gives the computed C_g (solid line) and S_θ (dashed line) integrated along time plotted versus period. The variation of C_g has four peaks over 0.4: P_1 =208 yr, P_2=278 yr, P_3=1050 yr, and P_4=1981 yr. Here, P_1 is one of the common periodicities between SSN and T, P_3 is close to the Eddy cycle (962 yr) of their common periodicity. For P_1 and P_2, their phase angle strengths (S_θ) are very low: $S_{\theta,p1}$=0.34 and $S_{\theta,p2}$=0.25. That means the variations of SSN and T are not phase-locked at these periodic components although the wavelet coherence between them is high. Sometimes the variation of SSN leads that of T; while for other times, the former lags the latter.

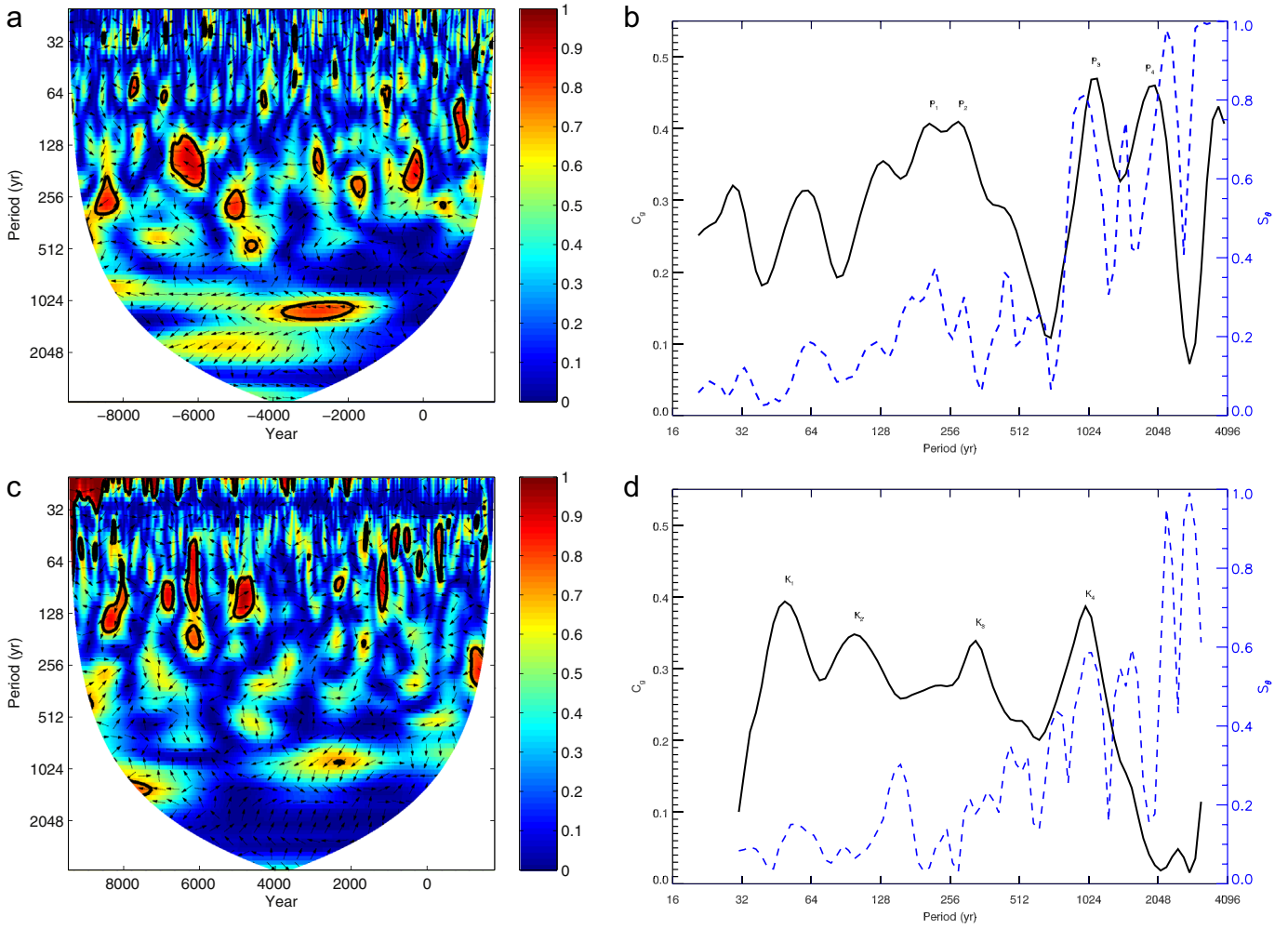

Fig. 2. (a) Squared wavelet coherence between the SSN and T time series. The thick black contours indicate the 95% confidence level against red noise. Black arrows represent phase angles of the cross wavelet (with in-phase pointing right, anti-phase pointing left, SSN leading T by 90° pointing straight down, and SSN lagging T by 90° pointing straight up). The regions inside COI are removed. (b) The global wavelet coherence (C_g, solid line) and the phase angle strength (S_θ, dashed line) between SSN and T plotted against period. (c) Same as (a) but for the CO_2 and T time series. (d) Same as (b) but for the CO_2 and T time series. (For interpretation of the references to color in this figure legend, the reader is referred to the web version of this article.)

Therefore, there are no stable connections between them at these periodicities. As to the peaks of P_3 and P_4, both C_g and S_θ are high ($C_{g,p3}=0.47$, $S_{\theta,p3}=0.77$; $C_{g,p4}=0.46$, $S_{\theta,p4}=0.75$). It means that not only SSN and T have high coherence, but also their variations are phase-locked at these periodicities. In other words, the components of SSN and T at these periods/frequencies may have both strong and stable connections.

Similarly, Fig. 2(c) displays the squared wavelet coherence between CO_2 and T, Fig. 2(d) shows their global wavelet coherence C_g (solid line) and phase angle strength S_θ (dashed line) outside COI plotted versus period. Comparing Fig. 2(c) with Fig. 2(a), we can find that the "islands" with wavelet coherence higher than the 95% confidence level between CO_2 and T are fewer than those between SSN and T. The period band with these high coherence "islands" between CO_2 and T lies approximately within [64, 256] yr, narrower than the band of [64, 512] yr between SSN and T. The variations of CO_2 and T at these periodicities are not phase-locked as well. For low frequency components around the period of 1024 yr, the area of the "island" is greatly reduced in contrast with Fig. 2(a); the phase arrows shifts from upward to downward as time (Year) increases. Fig. 2(d) demonstrates that the variation of C_g has four peaks: $K_1=49$ yr, $K_2=98$ yr, $K_3=331$ yr, and $K_4=991$ yr. The values of their global wavelet coherence and phase angle strengths are: $C_{g,k1}=0.39$, $S_{\theta,k1}=0.12$; $C_{g,k2}=0.35$, $S_{\theta,k2}=0.06$; $C_{g,k3}=0.34$, $S_{\theta,k3}=0.18$; $C_{g,k4}=0.39$, $S_{\theta,k4}=0.59$. Therefore, the variations of CO_2 and T are not phase-locked at the periods of K_1–K_3. As to K_4, the variations of CO_2 and T at this periodicity are locked better than those at K_1–K_3, but worse than the variations of SSN and T at P_4 ($S_{\theta,k4}=0.59<S_{\theta,p4}=0.75$).

In order to display the change of the phase angle more clearly, Fig. 3 gives the drawing of the phase arrows along time outside COI for the periodicities of P_1–P_4 between SSN and T (Fig. 3(a)) and K_1–K_4 between CO_2 and T (Fig. 3(b)). In this figure, arrows point straight right for $\theta=0°$, straight left for $\theta=\pm 180°$, down for $0°<\theta<180°$, and up for $-180°<\theta<0°$. Red arrows denote the phase angles with the wavelet coherence higher than the 95% confidence level against red noise. $\theta_{ave,\ p1}$–$\theta_{ave,\ p4}$ are the circular means of the phase angles outside COI for P_1–P_4, $\theta'_{ave,\ p1}$–$\theta'_{ave,\ p3}$ represent the circular mean of θ with wavelet coherence higher than the 95% confidence level outside COI for P_1–P_3. We see from Fig. 3(a) that arrows point to all directions for P_1 and P_2 with diversified arrow directions. For P_3, the arrows point neatly to the up-left direction during most time of the past 11,000 years, and the circular mean of the phase angles is $\theta_{ave,\ p3}=-170.0°\pm 41.7°$. For P_4, the arrows point regularly down with the circular mean of the phase angles $\theta_{ave,\ p4}=108.6°\pm 43.7°$. The phase angle can be converted to a lead/lag time for a specific wavelength (i.e.

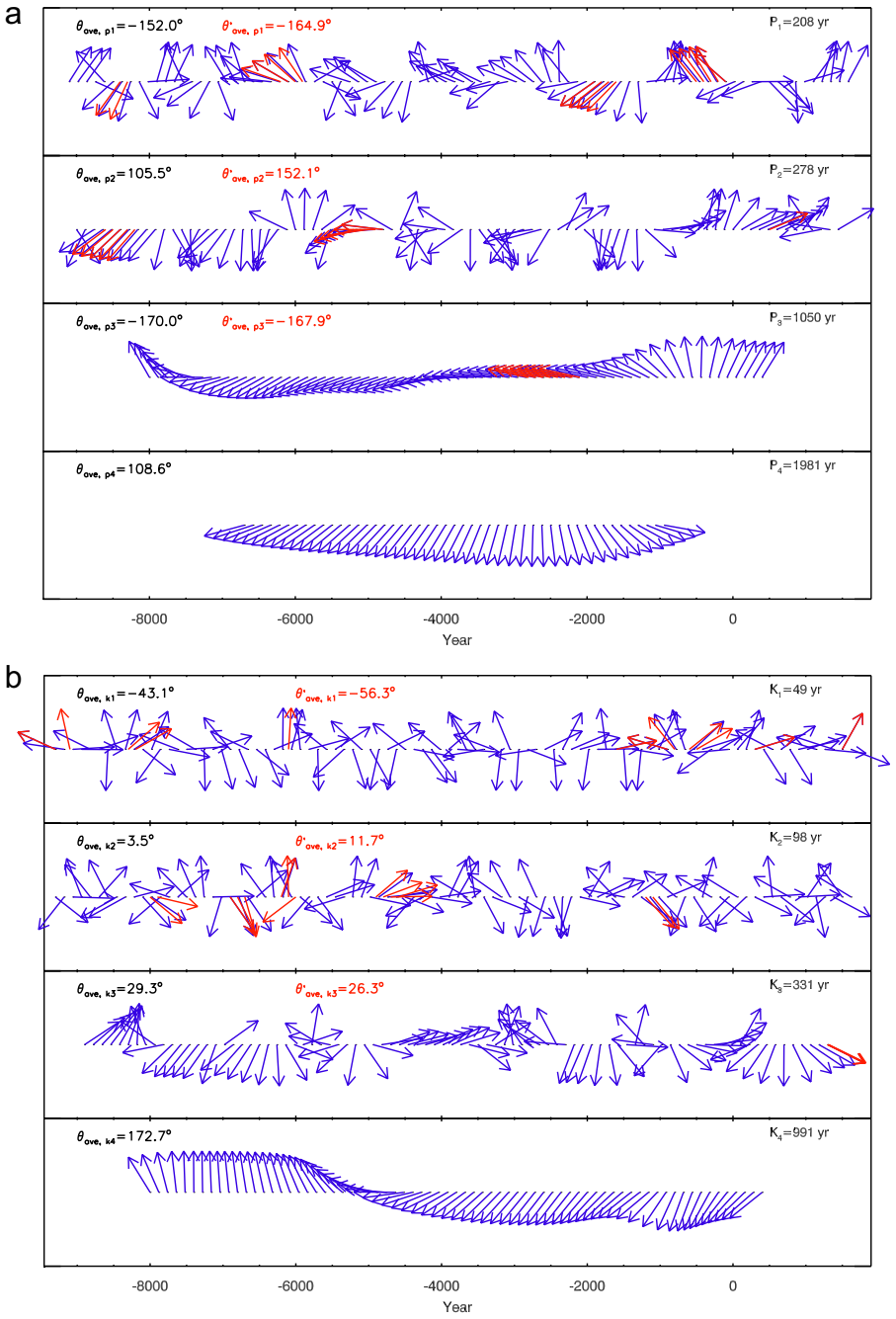

Fig. 3. (a) The variations of the relative phase angle (θ) of the wavelet coherence between SSN and T outside COI along time for the periodicities of P_1, P_2, P_3 and P_4. Arrows are pointing straight right for $\theta=0°$, pointing straight left for $\theta = \pm 180°$, pointing down for $0° < \theta < 180°$, and pointing up for $-180° < \theta < 0°$. Red arrows represent the phase angles with wavelet coherence higher than the 95% confidence level of red noise. θ_{ave} and θ'_{ave} are the circular means of all the phase angles outside COI and of the phase angles with wavelet coherence higher than the 95% confidence level outside COI, respectively. (b) The same as (a) but for the periodicities of K_1–K_4 between CO_2 and T. (For interpretation of the references to color in this figure legend, the reader is referred to the web version of this article.)

frequency/period):

$$\Delta T = \frac{\Delta\theta \times L_P}{360°} \tag{3}$$

Here, $\Delta\theta$ is the difference between the phase angle and the in-phase/anti-phase angle, L_p is the period length. $\Delta T > 0$ implies that the variation of SSN leads that of T, while $\Delta T < 0$ implies that the variation of SSN lags that of T. For P_3, the variation of the time series at this frequency is close to anti-phase ($-180°$), $\Delta\theta_{p3} = -170.0° - (-180°) = 10.0°$, $L_{p3}=1050$ yr, then $\Delta T_{p3}=29.2$ yr. Therefore, the variation of SSN leads that of T by 29.2 yr. As to P_4, the relative relation of SSN and T lies between in-phase and anti-phase. If we take the in-phase relation, $\Delta\theta_{p4}=108.6°-0°=108.6°$, $L_{p4}=1981$ yr, and $\Delta T_{p4}=597.6$ yr. The SSN leads T by 597.6 yr at this periodic component. It needs to be pointed out that this method of computing lead/lag time works best when the time series are close to in-phase/anti-phase. Re-considering the case of P_4, we can also say that SSN lags T by $1981/2-597.6=392.9$ yr with these two series in anti-phase relation. In other words, the relation between SSN and T at the 1981 yr periodic component is not as clear as the one at the 1050 yr periodic component.

In Fig. 3(b), arrows point to all directions for K_1–K_3,re-verifying the non-phase-locked relations between CO_2 and T at these periodicities. As to K_4, the arrows change from upward at left to

downward at right, which supports that the relation between CO_2 and T at this periodic component is also not as stable as the one between SSN and T at $P_3=1050$ yr. As a summary to Figs. 2 and 3, there are intermittent periodicities where the correlations between SSN and T are strong during the past 11,000 years before the modern industry. But these anti-correlations remain clear and stable only for the millennium-cycle component (1050 yr of period, close to the Eddy cycle of SSN). The variation of SSN leads that of T by about 29.2 yr. The correlations between CO_2 and T are weaker than those between SSN and T; no resonant cycle is found where the relation between CO_2 and T keeps strong and stable.

3.3. Millennial-scale variations

In order to display the evolutions of the millennial-scale components of SSN and T, we apply a band-pass-filter to the time series of SSN and T. The designed band-pass filter is centered at 1000 yr with half-power points at 1000 ± 100 yr. The center of 1000 yr is set between the Eddy cycle (962 yr, existing in SSN and T) and their strong coherence cycle ($P_3=1050$ yr). The evolutions of the millennial components of SSN and T output from the band-pass-filter are shown in Fig. 4(a). The anti-phase relation between SSN and T can be clearly seen from this figure, and this anti-phase relation keeps throughout the whole 11,000 years of the past. Fig. 4(b) gives the correlation coefficients between the millennial components of SSN and T plotted versus the lead time of SSN relative to T. It can be seen that their correlation reaches strongest when SSN leads T by 40 yr. The corresponding correlation coefficient is -0.85. This lead time is consistent with $\Delta T_{p3}=29.2$ yr obtained through the wavelet coherence analysis between SSN and T. The plot of SSN is shifted to right for 40 years in Fig. 4(a) in order to give the best match. One point to mention is that the variation of the millennial component of T mainly lies within [−0.2 °C, 0.2 °C]. While the variation of the total T in Fig. 1(b) occupies the range of [−1 °C, 1 °C]. Therefore, the millennial-scale change of T associated with solar variability may account for no larger than 20% of its total variance in general. We need to point out that it is only a very rough estimation.

However, the anti-correlation between SSN and T derived here indicates that higher SSN leads to lower T, which is contrary to the previously known evidences of higher SSN leading to higher temperature of the Earth (e.g., Bond et al., 2001; Usoskin et al., 2000; 2001; 2005; Usoskin and Kovaltsov, 2008; Eichler et al., 2009; Usoskin, 2011). This discrepancy can be interpreted as follow. The temperature that we used is only a local temperature in the inland Antarctica (Vostok). Changes of the local climate do not necessarily follow the global trend, and the differences of climate change trends between locations can be large (Trenberth et al., 2007). In fact, the climate in the Antarctic changed in anti-phase with that in the northern Atlantic on millennial scales during the last deglaciation, and this concept had been dubbed the “bipolar seesaw” (Broecker, 1998). Similarly, the millennial climate changes in the two polar regions of the Earth had been found to be anti-phased during the last glacial cycle (Blunier and Brook, 2001). Oceanic or atmospheric processes are believed to be possible explanations for these anti-correlations. For example, an increase in the North Atlantic thermohaline circulation would warm the high-latitude Northern Hemisphere and cool at least parts of the Southern Hemisphere on millennial scales (Stocker, 2000; Blunier and Brook, 2001). This bipolar see-saw was pointed out to be a persistent feature of the glacial climate, and the forcing of these millennial-scale climate changes was believed to arise in the Northern Hemisphere (Blunier and Brook, 2001). Denton and Broecker (2008) hypothesized that a meridional bipolar see-saw had been a pattern of the climate variability during the Holocene, which covers the time period of data in this study. Swingedouw et al. (2011) simulated the solar forcing of the climate during the last millennium by using a state-of-the-art climate mode. They found that the regional temperature response to the solar forcing was not uniform. Although an increased warming occurred in the Northern Hemisphere for the period AD 1001–AD 1860, a decreased warming occurred in the Southern Hemisphere with even a cooling from 50°S to the Southern Pole during that period. They pointed out that the increase in the zonal wind speed (and stress) between 40°S and 70°S should be a more plausible explanation to the anti-correlation (inverse relation) between the Southern

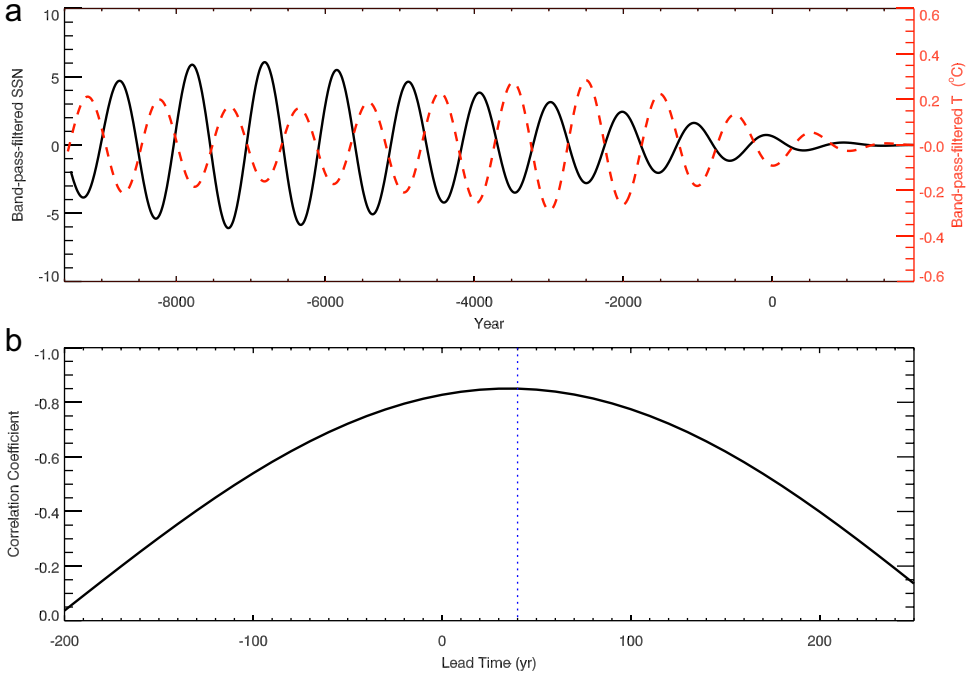

Fig. 4. (a) Evolutions of the millennial components of SSN and T along time computed from the band-pass-filter. The plot of SSN is shifted to right for 40 years. (b) The correlation coefficient between the millennial components of SSN and T plotted versus the lead time of SSN relative to T.

Hemisphere temperature and the solar forcing. Even at the present era, warming dominates most of the seasonal maps for the period AD 1979 onwards, but weak cooling has affected a few regions, especially the mid-latitudes of the Southern Hemisphere oceans, possibly through changes in atmospheric and oceanic circulation related to the Pacific Decadal Oscillation and Southern Annular Mode (Trenberth et al., 2007). Based on these evidences, we can infer reasonably that SSN and the Northern Hemisphere (even the global) temperature should be positive-correlated on millennial scales during the period that we investigated. Some kinds of climatic mechanisms, such as the complicated oceanic or atmospheric processes, led to the anti-correlation (inverse relation) between the millennial-scale changes of the Antarctic local temperature and the solar forcing. However, we have to remember that this is only a preliminary inference. Further studies should be focused on the phasing of the millennial-scale variations of the climate between the hemispheres as well as the phasing between solar activity and the global climate change in order to confirm this hypothesis.

4. Summary and conclusion

The Sun is the main energy source for the complicated climatic system of our Earth. Therefore, the solar forcing is believed to have an effect on the Earth's climate change. The debate as to how much solar activity could affect the Earth's climate has never stopped since its appearance. One of the reasons for this long debate is the relatively short length of continuous data of direct observations in both solar activity and climate change. In this paper, we employ the long reconstructed datasets of SSN, the local temperature and air CO_2 concentration in the inland Antarctica to investigate their variation periodicities and correlations during the past 11,000 years before modern industry. It is found that SSN and temperature have some common periodicities, such as the 208 (204) yr, 441 yr, 488 (483) yr, 521 (516) yr, 562 (568) yr and 962 yr cycles, during the interval of interest. The distributions of the Lomb–Scargle spectral periodograms of SSN and *T* are also similar. The consistence of their periodicities attracts us to further investigate the wavelet coherence between them. Corresponding results demonstrate that the overall coherence between SSN and *T* is not as strong as expected. Good correlations only exist for some intermittent periodicities and vary with time. The relative phases between SSN and *T* are not well locked for the period bands of 64–512 yr. However, the very low frequency variations of solar activity, denoted by the millennial component of SSN, have not only a good correlation but also a stable anti-phase relation with those of the local temperature in Vostok during the whole 11,000 years that we studied. The variation of SSN leads that of *T* by 30–40 yr. All these imply that the long-term variations of solar activity may have potential effects on the local climate change in Antarctica. As to the atmospheric CO_2 concentration, it has neither strong nor stable correlations with the local temperature change during the past 11,000 years of the pre-industrial time.

Our results are comparable to other studies based on similar reconstructed data. Bond et al. (2001) found evidences about the close correlation between inferred changes in production rates of the cosmogenic nuclides ^{14}C and ^{10}Be and centennial to millennial time scale changes in proxies of drift ice measured in deep-sea sediment cores. They pointed out that a solar forcing mechanism should underlie at least the Holocene segment of the North Atlantic's "1500-year" cycle. Usoskin et al. (2005) compared the reconstructed series of SSN, cosmic ray flux and the terrestrial Northern Hemisphere mean surface temperatures over time intervals of up to nearly 1800 years, and revealed consistently positive correlations for SSN and negative correlations for the cosmic rays in contrast with the temperature. The significance levels, as pointed out by them, vary strongly for the different data sets. Eichler et al. (2009) used the ice core oxygen isotope record from the continental Siberian Altai as a high-resolution temperature proxy for the last 759 years. They found strong correlation between the reconstructed temperature and solar activity, suggesting the solar forcing as a main driver for temperature variations in the Altai region during the pre-industrial time (AD 1250–AD 1850). They identified a 10–30 year lag between the solar forcing and the temperature response, and also obtained that the reconstructed temperature was not significantly correlated with the greenhouse gas CO_2. More recently, Zhao and Feng (2014) investigated the periodicities and correlations between solar activity and the Earth's temperature on centennial scales based on the measured SSN, the reconstructed total solar irradiance (TSI) and the observed surface temperature of the Earth. They found that SSN and the Earth's temperature had a common periodicity of 50 yr during the period AD 1880–AD 2012, and the variation of solar activity led that of the Earth's temperature. However, it is difficult to determine the quantitative role of solar activity on the Earth's climate change at present. More evidences need to be found to better understand the long term impact of solar activity on the climate change of our Earth.

Acknowledgments

This work is supported by the National Basic Research Program (973 program) under grant 2012CB825601, the Knowledge Innovation Program of the Chinese Academy of Sciences (KZZD-EW-01-4), the National Natural Science Foundation of China (41031066, 41231068, 41274179, 41174150, 41474153), and the "Five key cultivation directions" Fund of the National Space Science Center Chinese Academy of Sciences. Thanks go to Dr. J P Guo for beneficial discussions on data analysis methods. Thanks also go to Dr. C Q Xiang for verifying the English writing of the paper.

References

Herschel, W., 1801. Observations tending to investigate the nature of the Sun, in order to find the causes or symptoms of its variable emission of light and heat: With remarks on the use that may possibly be drawn from solar observations. Philos. Trans. R. Soc. Lond. 91, 265–318.

Eddy, J.A., 1976. The Maunder Minimum. Science 192, 1189–1202.

Currie, R.G., 1979. Distribution of solar cycle signal in surface air temperature over North America. J. Geophys. Res. 84, 753–762.

Friis-Christensen, E., Lassen, K., 1991. Length of the solar cycle: an indicator of solar activity closely associated with climate. Science 254, 698–700.

Lean, J., Beer, F., Bradley, R., 1995. Reconstruction of solar irradiance since 1610: implications for climate change. Geophys. Res. Lett. 22, 3195–3198.

Hegerl, G.C., Zwiers, F.W., Braconnot, P., Gillett, N.P., Luo, Y., Marengo Orsini, J.A., Nicholls, N., Penner, J.E., Stott, P.A., 2007. Understanding and attributing climate change. In: Solomon, S., Qin, D., Manning, M., Chen, Z., Marquis, M., Averyt, K.B., Tignor, M., Miller, H.L. (Eds.), Climate Change 2007: The Physical Science Basis. Contribution of Working Group I to the Fourth Assessment Report of the Intergovernmental Panel on Climate Change. Cambridge University Press, Cambridge, United Kingdom and New York, NY, USA.

Bond, G., Kromer, B., Beer, J., Muscheler, R., Evans, M.N., Showers, W., Hoffmann, S., Lotti-Bond, R., Hajdas, I., Bonani, G., 2001. Persistent solar influence on north Atlantic climate during the Holocene. Science 294, 2130–2135.

Usoskin, I.G., Schüessler, M., Solanki, S.K., Mursula, K., 2005. Solar activity, cosmic rays, and Earth's temperature: a millennium-scale comparison. J. Geophys. Res. 110, A10102. http://dx.doi.org/10.1029/2004JA010946.

Scafetta, N., West, B.J., 2006. Phenomenological solar contribution to the 1900–2000 global surface warming. Geophys. Res. Lett. 33, L05708. http://dx.doi.org/10.1029/2005GL025539.

Svensmark, H., 2007. Cosmoclimatology: a new theory emerges. Astron. Geophys. 48, 118–124.

Singer, S.F., 2008. Nature, not human activity, rules the climate. Cambridge University Press, Cambridge, UK, pp. 1–40.

Eichler, A., Olivier, S., Henderson, K., Laube, A., Beer, J., Papina, T., Gäggeler, H.W., Schwikowski, M., 2009. Temperature response in the Altai region lags solar

forcing. Geophys. Res. Lett. 36, L01808. http://dx.doi.org/10.1029/2008GL035930.
Ziskin, S., Shaviv, N.J., 2012. Quantifying the role of solar radiative forcing over the 20th century. Adv. Space Res. 50, 762–776.
Usoskin, I.G., 2013. A history of solar activity over millennia. Living Rev. Sol. Phys. 10, 1–94. http://dx.doi.org/10.12942/lrsp-2013-1.
Solanki, S.K., Usoskin, I.G., Kromer, B., Schüssler, M., Beer, J., 2004. Unusual activity of the Sun during recent decades compared to the previous 11,000 years. Nature 431, 1084–1087.
Petit J.R. et al., 2001, Vostok ice core data for 420,000 years. IGBP PAGES/World Data Center for Paleoclimatology Data Contribution Series #2001-076, NOAA/NGDC Paleoclimatology Program, Boulder CO, USA.
Petit, J.R., Jouzel, J., Raynaud, D., Barkov, N.I., Barnola, J.M., Basile, I., Bender, M., Chappellaz, J., Davis, J., Delaygue, G., Delmotte, M., Kotlyakov, V.M., Legrand, M., Lipenkov, V., Lorius, C., Pépin, L., Ritz, C., Saltzman, E., Stievenard, M., 1999. Climate and atmospheric history of the past 420,000 years from the Vostok ice core, Antarctica. Nature 399, 429–436.
Monnin, E., Steig, E.J., Siegenthaler, U., Kawamura, K., Schwander, J., Stauffer, B., Stocker, T.F., Morse, D.L., Barnola, J.-M., Bellier, B., Raynaud, D., Fischer, H., 2004. Evidence for substantial accumulation rate variability in Antarctica during the Holocene, through synchronization of CO2 in the Taylor Dome, Dome C and DML ice cores. Earth Planet. Sci. Lett. 224, 45–54. http://dx.doi.org/10.1016/j.epsl.2004.05.007.
Lomb, N.R., 1976. Least-squares frequency analysis of unequally spaced data. Astrophys. Space Sci. 39, 447–462.
Scargle, J.D., 1982. Studies in astronomical time series analysis. II. Statistical aspects of spectral analysis of unevenly spaced data. Astrophys. J. 263, 835–853.
Torrence, C., Compo, G.P., 1998. A practical guide to wavelet analysis. Bull. Am. Meteorol. Soc. 79, 61–78.
Grinsted, A., Moore, J.C., Jevrejeva, S., 2004. Application of the cross wavelet transform and wavelet coherence to geophysical time series. Nonlin. Process. Geophys. 11, 561–566.
Suess, H.E., 1980. The radiocarbon record in tree rings of the last 8000 years. Radiocarbon 22, 200–209.
Abreu, J.A., Beer, J., Ferriz-Mas, A., McCracken, K.G., Steinhilber, F., 2012. Is there a planetary influence on solar activity? Astron. Astrophys. 584, A88.
McCracken, K.G., Beer, J., Steinhilber, F., Abreu, J., 2013a. A phenomenological study of the cosmic ray variations over the past 9400 years, and their implications regarding solar activity and the solar dynamo. Sol. Phys. 286, 609–627.
McCracken, K.G., Beer, J., Steinhilber, F., 2014. Evidence for planetary forcing of the cosmic ray intensity and solar activity throughout the past 9400 years. Sol. Phys. 289, 3207–3229.
Steinhilber, F., Beer, J., 2013. Prediction of solar activity for the next 500 yearsJ. Geophys. Res. Space Phys. 118, 1861–1867.
Steinhilber, F., Abreu, J.A., Beer, J., McCracken, K., 2010. The interplanetary magnetic field during the past 9300 years inferred from cosmogenic radionuclides. J. Geophys. Res. 115, A01104.
McCracken, K., Beer, J., Steinhilber, F., Abreu, J., 2013b. The heliosphere in time. Space Sci. Rev. 176, 59–71.
Lüdecke, H.J., Hempelmann, A., Weiss, C.O., 2013. Multi-periodic climate dynamics: spectral analysis of long-term instrumental and proxy temperature records. Clim. Past 9, 447–452.
Usoskin, I.G., Mursula, K., Kovaltsov, G.A., 2000. Cyclic behaviour of sunspot activity during the Maunder minimum. Astron. Astrophys. 354, L33–L36.
Usoskin, I.G., Mursula, K., Kovaltsov, G.A., 2001. Heliospheric modulation of cosmic rays and solar activity during the Maunder minimum. J. Geophys. Res. 106, 16039–16046.
Usoskin, I.G., Kovaltsov, G.A., 2008. Cosmic rays and climate of the Earth: possible connection. Comptes Rendus Geosci. 340, 441–450.
Usoskin, I.G., 2011. Cosmic rays and climate forcing. Mem. Soc. Astron. Ital. 82, 937–942.
Trenberth, K.E., Jones, P.D., Ambenje, P., Bojariu, R., Easterling, D., Tank, A.K., Parker, D., Rahimzadeh, F., Renwick, J.A., Rusticucci, M., Soden, B., Zhai, P., 2007. Observations: surface and atmospheric climate change. In: Solomon, S.,D., Qin, M., Manning, Z., Chen, M., Marquis, K.B., Averyt, M., Tignor, Miller, H.L. (Eds.), Climate Change 2007: The Physical Science Basis. Contribution of Working Group I to the Fourth Assessment Report of the Intergovernmental Panel on Climate Change. Cambridge University Press, Cambridge, United Kingdom and New York, NY, USA.
Broecker, W.S., 1998. Paleocean circulation during the last deglaciation: a bipolar seesaw? Paleoceanography 13, 119–121.
Blunier, T., Brook, E.J., 2001. Timing of millennial-scale climate change in Antarctica and Greenland during the last glacial period. Science 291, 109–112.
Stocker, T.F., 2000. Past and future reorganizations in the climate system. Quat. Sci. Rev. 19, 301–319.
Denton, G.H., Broecker, W.S., 2008. Wobbly ocean conveyor circulation during the Holocene? Quat. Sci. Rev. 27, 1939–1950.
Swingedouw, D., Terray, L., Cassou, C., Voldoire, A., Salas-Mélia, D., Servonnat, J., 2011. Natural forcing of climate during the last millennium: fingerprint of solar activity. Clim. Dyn 36, 1349–1364.
Zhao, X.H., Feng, X.S., 2014. Periodicities of solar activity and the surface temperature variation of the Earth and their correlations. Chin. Sci. Bull. (Chin. Ver.) 59, 1284–1292(Chinese Version).